

# **The sarcoplasmic-endoplasmic reticulum $\text{Ca}^{2+}$ -ATPase (SERCA) is the likely molecular target for the acute toxicity of the brominated flame retardant hexabromocyclododecane (HBCD).**

Fawaz Al-Mousa and Francesco Michelangeli\*

School of Biosciences  
University Of Birmingham  
Edgbaston  
Birmingham  
UK  
B15 2TT

\* Corresponding Author: F. Michelangeli  
F.Michelangeli@Bham.ac.uk  
Tel: +44-1214145398  
Fax: +44-1214145925  
Address as above

## **Keywords**

Hexabromocyclododecane; brominated flame retardant; SERCA  $\text{Ca}^{2+}$  pumps

## **Abbreviations**

Brominated flame retardants, BFRs; Hexabromocyclododecane, HBCD, Sarcoplasmic-endoplasmic reticulum  $\text{Ca}^{2+}$  ATPase, SERCA; Tetrabromobisphenol-A, TBBPA.

**Abstract**

Hexabromocyclododecane (HBCD) is a widely utilised brominated flame retardant (BFR). It has been shown to bio-accumulate within organisms, including man, and possibly cause neurological disorders. The acute neurotoxicity of HBCD, and 6 other unrelated BFRs, were assessed in SH-SY5Y human neuroblastoma cells by 24 hour viability assays and HBCD proved to be the most lethal ( $LC_{50}$ ,  $3\mu\text{M}$ ). In addition, the effects of these BFRs were also assessed for their potency at inhibiting the sarcoplasmic-endoplasmic reticulum  $\text{Ca}^{2+}$  ATPase (SERCA) derived from the SH-SY5Y cells and again HBCD was the most potent ( $IC_{50}$ ,  $2.7\mu\text{M}$ ). The data for the other BFRs tested showed a direct correlation (coefficient 0.94) between the potencies of inducing cell death and inhibiting the  $\text{Ca}^{2+}$  ATPase, indicating that SERCA is likely to be the molecular target for acute toxicity. Mechanistic studies of HBCD on the  $\text{Ca}^{2+}$  ATPase suggest that it affects ATP binding, phosphorylation as well as the E2 to E1 transition step.

## 1.0 **Introduction**

$\text{Ca}^{2+}$  is a commonly employed signal within cells that regulates many different cellular processes such as contraction, secretion, neurotransmission, proliferation and death by increasing intracellular  $\text{Ca}^{2+}$  concentrations ( $[\text{Ca}^{2+}]_i$ ) levels [1]. Inadequate or prolonged elevation of  $[\text{Ca}^{2+}]_i$  may lead to deleterious effects [1] and to avoid these effects,  $[\text{Ca}^{2+}]_i$  levels must be strictly controlled by a variety of  $\text{Ca}^{2+}$  transporters including the sarcoplasmic-endoplasmic reticulum  $\text{Ca}^{2+}$  ATPase (SERCA)  $\text{Ca}^{2+}$  pumps [1,2], which help to maintain low cytosolic  $[\text{Ca}^{2+}]_i$  levels. Therefore agents which have inhibitory effects on these  $\text{Ca}^{2+}$  pumps will have harmful consequences to cells and tissues [2].

1,2,5,6,9,10-Hexabromocyclododecane (HBCD) is a cyclic aliphatic brominated flame retardant (BFR) and is one of the major BFRs produced and used today. The main application of HBCD is in polystyrene foam that is used in thermal insulation of building materials, electronics, textiles and upholstered furniture.

A number of brominated flame retardants (BFRs), including 1,2,5,6,9,10-hexabromocyclododecane (HBCD), have recently been recognized as widespread environmental contaminants which are able to bio-accumulate within living organisms, including man [3]. In humans, the major intake of HBCD is from food, indoor air and dust [4]. High concentrations of up to 19200 ng/g lipid weight (lw) were found in the blood of birds of prey (equivalent to 12  $\mu\text{M}$ ) and more than 9600 ng/g lw in marine mammals (equivalent to 6  $\mu\text{M}$ ) [5]. In addition, concentrations of 850 ng/g lw (equivalent to 0.5  $\mu\text{M}$ ) were found in some human blood samples [6] as well as also being reported in human milk [7]. A number of BFRs including HBCD have been shown to be specifically neurotoxic in nature, causing neuronal cell death [3,8] and having detrimental effects on brain development, leading to adverse effects on behaviour, learning and memory [9].

It is clear that some of BFRs are able to elicit increases in intracellular  $[\text{Ca}^{2+}]_i$ , which can lead to cellular dysfunction and cell death in a variety of cells types including neurons [3,8, 11-13]. Recently our group has shown that Tetrabromobisphenol A is

able to inhibit the SERCA  $\text{Ca}^{2+}$  pumps at low micromolar ( $\mu\text{M}$ ) concentrations within a range of cell types [2,8,11]. Mobilisation of intracellular  $\text{Ca}^{2+}$  stores by inhibiting SERCA activity is one of the mechanisms by which BFRs (like other hydrophobic environmental pollutants) interfere with the  $\text{Ca}^{2+}$  signalling pathway and cause cell death [8,10,11].

It is now evident that a number of BFRs are cytotoxic at low  $\mu\text{M}$  concentrations within cells by altering intracellular  $[\text{Ca}^{2+}]$  levels [8,11-13]. This has led us to investigate the effects of HBCD on SERCA  $\text{Ca}^{2+}$  pumps in order to determine the likelihood of it being the molecular target for acute toxicity and additionally elucidate the molecular mechanism by which this BFR causes its effect upon this  $\text{Ca}^{2+}$  transporter.

## **2.0 Materials and Methods**

### **2.1 Chemicals**

1,2,5,6,9,10-Hexabromocyclododecane (HBCD) (purity > 95%, commercial grade which is typically 82%  $\gamma$ -isomer and 12%  $\alpha$ -isomer), Dibromobiphenyl (DBBP) (98% purity), decabromodiphenyl ether (DBPE) (>99% purity) and tetrabromobisphenol-A diallyl ether (TBBPA-DAE) (>99% purity) were purchased from Sigma-Aldrich Co. Ltd, UK. Tetrabromobisphenol-A (TBBPA) (97% purity) was purchased from Acros Organics, UK. Pentabromodiphenyl ether (PBDE) and Octabromodiphenyl ether (OBDE) (both >98% purity) were purchased from Wellington Laboratories Inc., Canada. MTT (3-(4,5-Dimethyl-2-thiazolyl)-2,5-diphenyl-2H-tetrazolium bromide thiazole blue) was purchased from Sigma-Aldrich co. Ltd., UK All other reagents were of analytical grade.  $[\gamma\text{-}^{32}\text{P}]$  ATP was obtained from Amersham, UK.

### **2.2 Cell culture**

The SH-SY5Y human neuroblastoma cell line, were grown in Dulbecco's modified Eagle's medium (DMEM) supplemented with 2 mM L-glutamine, 1% penicillin (20 units/ml), streptomycin (20 mg/ml), and supplemented with 10% (vol/vol) heat-inactivated foetal bovine serum (FBS). Cells were maintained at 37 °C in a saturated humidity atmosphere containing 95% air and 5%  $\text{CO}_2$ .

### 2.3 MTT cell viability assays

SH-SY5Y neuronal cells were seeded in 24-well cell plates ( $4 \times 10^4$  cells/well) and allowed to cell grow at 37 °C until 80-90% confluency was reached. Pre-treatment with drug was undertaken in the culture medium with DMEM (high glucose/without phenol or FBS). Stock solutions of compounds were prepared by dissolving them in DMSO. The cells were exposed to varying concentrations of the compounds for 24h and the volume of DMSO did not exceed 1% of the total volume added to cells, which had little effect on viability. Cell viability was determined by MTT assay, using thiazolyl blue tetrazolium bromide (MTT reagent) as described in [11]. Viable cells form an intracellular formazan product when incubated with MTT reagent for 2-3h, and this product was then solubilised with 1ml acidic isopropanol and quantified spectroscopically by measuring the difference in absorbance ( $\Delta A = A_{570} - A_{650}$ ) and compared to cells not exposed to compounds (but with up to 1% DMSO alone).

### 2.4 Membranes preparation

SR  $\text{Ca}^{2+}$ -ATPase were prepared from rabbit skeletal muscle as described by Michelangeli and Munkonge (1991) [14]. Microsomal membranes were prepared from SH-SY5Y cells as described in [8]. Briefly, SH-SY5Y cells ( $1 \times 10^6$  cells/cm<sup>2</sup>) detached from the tissue flask, harvested by centrifugation at 1,000g for 10 min 4°C and washed with PBS. They were homogenized using a Teflon Potter-Elvehjem homogenizer in 10 vol. of buffer containing 300 mM sucrose and 5 mM Hepes, pH 7.2, in the presence of 0.1 mM PMSF, 10  $\mu\text{M}$  leupeptin and 100  $\mu\text{M}$  benzamidine, and then centrifuged for 10 min at 1000 g. The pellet was resuspended in 5 vol. of the same buffer re-homogenized and centrifuged as above. The resulting supernatants were pooled and centrifuged for 20 min at 10,000 g. The supernatant from this stage was centrifuged for 1 h at 100,000 g and the resulting pellet (microsomal membrane) was re-suspended in fresh Hepes / sucrose buffer, snap-frozen in liquid nitrogen and stored at -80 °C until use.

### 2.5 Measurement of the Ca<sup>2+</sup>-ATPase activity

The ATPase activity of the SR Ca<sup>2+</sup>ATPase was monitored using the coupled enzyme assay where the oxidation of NADH is coupled to hydrolysis of ATP via pyruvate kinase and lactate dehydrogenase, as described in [14,15]. All experiments were undertaken at 25° C and pH 7.2. In all experiments, excluding those where free [Ca<sup>2+</sup>] was altered, the optimal free [Ca<sup>2+</sup>] of 6 µM was used. In all experiments, excluding those where [ATP] was altered, 2.1mM [ATP] was used, and in all experiments, except those where [Mg<sup>2+</sup>] was altered, 5mM [Mg<sup>2+</sup>] was used. All three components are required in the assay in order to measure detectable levels of activity.

The Ca<sup>2+</sup>-dependent ATPase activity of SH-SY5Y cell microsomal membranes was performed using the phosphate liberation assay as described in Wootton and Michelangeli (2006) [16]. Briefly, microsomal extracts (5 µg) were re-suspended in 200 µl of buffer containing 45 mM HEPES/KOH (pH 7.0), 6 mM MgCl<sub>2</sub>, 2 mM NaN<sub>3</sub>, 250 mM sucrose, 12.5 µg/ml A23187 ionophore, and EGTA with CaCl<sub>2</sub> added to give a free [Ca<sup>2+</sup>] of 1 µM. Assays were pre-incubated at 37 °C for 10 minutes prior to activation with ATP (final concentration 6 mM) to initiate activity. The reaction was stopped after 40 minutes by addition of 50 µl 6.5% (w/v) trichloroacetic acid (TCA). The samples were put on ice for 10 min before centrifugation for 10 min at 14,000 g. The supernatant (100 µl) was added to 150 µl buffer containing (11.25% (v/v) acetic acid, 0.25% (w/v) copper sulphate, and 0.2 M sodium acetate pH 4.0). Ammonium molybdate (25 µl of 5% (w/v)) was then added, followed by the addition on 25 µl of *p*-methyl-aminophenol sulphate solution (2% (w/v) containing 5% (w/v) sodium sulphate). The samples were mixed and the blue colouration was allowed to develop for 10 min prior to measuring the absorption at 870 nm using a Dynatech Laboratories ELISA plate reader. The amount of Pi liberated was determined by comparison with known phosphate standards. The activities were also determined in the absence of Ca<sup>2+</sup> (1mM EGTA) to determine non Ca<sup>2+</sup>-dependent ATPase activity.

### 2.6 Phosphorylation studies

Phosphorylation of SR Ca<sup>2+</sup> ATPase by [ $\gamma$ -<sup>32</sup>P] ATP was carried out at 25 °C as described in [2]. The SERCA was diluted to 0.1 mg/ml in 40 mM Hepes/Tris (pH 7.2) containing 100 mM KCl, 5 mM MgSO<sub>4</sub>, 1 mM CaCl<sub>2</sub>, BSA (final conc. 1 mg/ml) and

12.5  $\mu\text{g/ml}$  A23187 in a total volume of 1 ml. The reaction was started by the addition of [ $\gamma$ - $^{32}\text{P}$ ] ATP from a stock (ATP concentration; 0.5 mM and specific radioactivity of 10 Ci/ mol) such that the samples contained between 0 and 20  $\mu\text{M}$  ATP. The reaction was then stopped by the addition of 250 $\mu\text{l}$  ice-cold 40% (w/v) TCA after 15s. The samples were placed on ice for 30 min. SR  $\text{Ca}^{2+}$ -ATPase was separated from the solution by filtration through Whatman GF/C filters. The filters were washed with 30 ml of 12.5 % (w/v) TCA containing 0.2 M  $\text{H}_3\text{PO}_4$  and left to dry. The filters were placed in scintillant and counted.

### 2.7 FITC-labelling of the $\text{Ca}^{2+}$ -ATPase to monitor E2 to E1 step

SR  $\text{Ca}^{2+}$ -ATPase was labelled with fluorescein 5'-isothiocyanate (FITC), according to the method described by Michelangeli et al. (1990) [17], to monitor the E2  $\rightarrow$  E1 transition. The  $\text{Ca}^{2+}$ -ATPase (1.1 mg/ml) was added in equal volume to the starting buffer (1 mM KCl 250 mM sucrose and 50 mM potassium phosphate pH 8.0). FITC in dimethylformamide was then added at a molar ratio of FITC/ATPase of 0.5: 1). The reaction was incubated for 1h at 25  $^{\circ}\text{C}$  and stopped by the addition of 250 $\mu\text{l}$  of stopping buffer (0.2 M sucrose, 50 mM Tris/HCl pH 7.0), which was left to incubate for 30 min at 30  $^{\circ}\text{C}$  prior to being placed on ice until required. Fluorescence measurements of FITC-ATPase were made in a buffer containing 50 mM Tris, 50 mM maleate, 5 mM  $\text{MgSO}_4$  and 100 mM KCl at pH 6.0. Fluorescence was measured in a Perkin Elmer LS50B fluorescence spectrophotometer at 25  $^{\circ}\text{C}$  (excitation 495 nm, emission 525 nm).  $\text{Ca}^{2+}$  (400  $\mu\text{M}$ ) was then added to induce changes in fluorescence intensity.

## 3.0 Results

### 3.1 Inhibition of $\text{Ca}^{2+}$ - ATPase activity and correlation with cell viability

Figure 1A shows effect of HBCD on the skeletal muscle SR SERCA 1A isoform of  $\text{Ca}^{2+}$  -ATPase activity, measured at pH 7.2 at 25 $^{\circ}\text{C}$ . HBCD inhibits the  $\text{Ca}^{2+}$ - ATPase with an  $\text{IC}_{50}$  values calculated to be  $2.7 \pm 0.6 \mu\text{M}$ . Figure 1A also shows the effects of HBCD on  $\text{Ca}^{2+}$ - ATPase activity in SH-SY5Y neuronal cell microsomal membranes which expresses mainly SERCA isoform 2B [18]. The  $\text{IC}_{50}$  value for inhibition was similar to that of skeletal muscle SERCA 1A, indicating that the inhibition of the  $\text{Ca}^{2+}$

ATPase was not isoform-specific. Figure 1B shows the  $IC_{50}$  for  $Ca^{2+}$  ATPase inhibition determined in SH-SY5Y cell microsomes for a range of BFRs. It can be seen that all the BFRs tested in this study inhibited the  $Ca^{2+}$ ATPase activity, although to different extents, ranging from  $IC_{50}$  values of 2.7  $\mu$ M for HBCD (which was the most potent BFR at inhibition  $Ca^{2+}$  ATPase) to 460  $\mu$ M for Dibromobiphenyl (DBBP). Of the brominated diphenyl ether BFRs tested, the highly brominated decabromodiphenylether (DBDE) was more potent at inhibiting the  $Ca^{2+}$  ATPase than the less brominated PBDE or OBDE. Figure 1B also shows the  $LC_{50}$  concentrations for the BFRs at inducing cell death in the SH-SY5Y neuronal cells, using the MTT cell viability assay. Figure 1B shows a direct relationship (correlation coefficient of 0.94) between potency of the BFRs at inhibiting the  $Ca^{2+}$ ATPase from the SH-SY5Y cells and their ability to induce cell death.

### 3.2 The effects of HBCD on SR $Ca^{2+}$ -ATPase (SERCA1A) activity as a function of $[Ca^{2+}]$ , $[ATP]$ and $[Mg^{2+}]$

As there is little difference in the potency of HBCD in inhibiting both the SERCA 1A isoform found abundantly in skeletal muscle and the SERCA 2B isoform found in neuronal cells, the highly abundant skeletal muscle form was used to further determine of the mode of inhibition of HBCD.

Figure 2A shows the effect of free  $[Ca^{2+}]$  on SERCA 1A  $Ca^{2+}$  ATPase activity measured at pH 7.2 and 25°C, in the absence and presence of 3  $\mu$ M HBCD. The Effects of free  $[Ca^{2+}]$  on  $Ca^{2+}$  ATPase activity shows a typical bell-shaped profile. The stimulatory phase of the curve, at low  $Ca^{2+}$  concentrations reflects  $Ca^{2+}$  binding to the E1 form (denoted by  $K_s$ ), while the inhibition part at higher  $Ca^{2+}$  concentrations reflects, in part,  $Ca^{2+}$  binding to the E2 conformation (denoted by  $K_i$ ) [2]. In the absence of HBCD the ATPase had a  $V_{max}$  of  $5.26 \pm 0.41$  IU/mg, with the  $K_s$  for the stimulatory phase of  $6.1 \times 10^{-7} \pm 1.3 \times 10^{-7}$  M, and a  $K_i$  value of  $1.2 \times 10^{-4} \pm 3 \times 10^{-5}$  M for the inhibitory phase (goodness-of-fit:  $\chi^2$  was 0.97). In the presence of HBCD (3 $\mu$ M), the data fitted to a  $V_{max}$  of  $2.79 \pm 0.26$  IU/mg, and stimulatory  $K_s$  and inhibitory  $K_i$  values  $5.5 \times 10^{-7} \pm 1.5 \times 10^{-7}$  M and  $1.8 \times 10^{-4} \pm 6 \times 10^{-5}$  M, respectively (goodness-of-fit:  $\chi^2$  was 0.97). These results suggest that there is little affect on the  $K_m$ s for  $Ca^{2+}$  binding but rather HBCD greatly affects the  $V_{max}$ .



Figure 2B, shows the activity of ATPase activity at varying ATP concentrations in the absences and presence of 3  $\mu\text{M}$  HBCD. The data for the SR  $\text{Ca}^{2+}$ -ATPase activity in the presence and absence of HBCD shows a biphasic profile which can be fitted to a bi-Michaelis-Menton Equation [2], assuming two independent ATP binding sites designated the high affinity catalytic site and the lower affinity regulatory site. The kinetic parameters for best fit; in the absence of HBCD was for the catalytic  $K_m = 6.3 \times 10^{-7} \pm 2.5 \times 10^{-7}$  M with a  $V_{\max}$   $1.42 \pm 0.13$  of IU/mg and a regulatory  $K_m$  and  $V_{\max}$  of  $0.00162 \pm 0.009$  M and  $4.52 \pm 1.34$  IU/mg, respectively. In presence of 3  $\mu\text{M}$  HBCD, the data could be fitted assuming, the  $K_m$ 's for both catalytic and regulatory sites were  $1.9 \times 10^{-6} \pm 6 \times 10^{-7}$  M and  $4.0 \times 10^{-4} \pm 3.6 \times 10^{-4}$  M, respectively. The  $V_{\max}$  values, however, were  $5.76 \pm 0.31$  IU/mg for the regulatory and catalytic  $V_{\max}$  value were  $1.63 \pm 0.13$  IU/mg, respectively (goodness-of-fit for the data sets;  $\text{Chi}^2$  were 0.98). These results indicate that HBCD causes a 3-fold decrease for the high affinity for catalytic ATP binding and an increase in affinity for the regulatory ATP binding site.

Figure 2C shows the effects of 3  $\mu\text{M}$  HBCD on SR  $\text{Ca}^{2+}$  ATPase activity as a function of  $[\text{Mg}^{2+}]$ . The ATPase activity decreases with increasing concentrations of  $\text{Mg}^{2+}$  both in the absence and presence of HBCD. The  $\text{IC}_{50}$  of  $[\text{Mg}^{2+}]$  upon  $\text{Ca}^{2+}$ -ATPase activity in the absence and presence of HBCD was  $3.3 \pm 0.5$  mM and  $4.3 \pm 0.8$  mM, respectively, whereas the  $V_{\max}$  decreased from  $6.3 \pm 0.7$  IU/mg to  $3.4 \pm 0.4$  IU/mg (goodness-of-fit:  $\text{chi}^2$  were 0.99 and 0.98, respectively). As  $\text{Mg}^{2+}$  inhibits the luminal dissociation of  $\text{Ca}^{2+}$  from the E2 phosphorylated state of the  $\text{Ca}^{2+}$ -ATPase [19], the data therefore suggests that HBCD causes little affect upon the E2 phosphorylated state.

### 3.3 The effects of HBCD on the phosphorylation of ATPase by ATP

In order to further assess the possible effect of HBCD on the ATP binding and the phosphorylation step of  $\text{Ca}^{2+}$ -ATPase,  $^{32}\text{P}$ -ATP phosphorylation experiments were performed with range ATP concentrations (0, 2.5, 5, 10 and 20  $\mu\text{M}$ ) in the absence and presence of 10  $\mu\text{M}$  HBCD. As shown in figure 3, HBCD caused a decrease in the phosphorylation level of the  $\text{Ca}^{2+}$  ATPase as a function of  $[\text{ATP}]$ . The data could be fitted to a single-site binding curve, with an  $\text{E-P}_{\max}$  and  $K_d$  for the control data of  $6.3 \pm$

1.7 nmol/mg and  $0.2 \pm 0.02 \mu\text{M}$ , respectively. Whereas in the presence  $10 \mu\text{M}$  HBCD, the data gave an  $E\text{-P}_{\text{max}}$  and  $K_d$  values of  $6.5 \pm 1.4 \text{ nmol/mg}$  and  $3.2 \pm 0.8 \mu\text{M}$ , respectively. This result indicates that HBCD causes a decrease in the ATP binding affinity to the  $\text{Ca}^{2+}$ -ATPase rather than on the maximal phosphorylation level.

### 3.4 The effects of HBCD on the E2 / E1 transition step

To determine whether HBCD affects the E2 / E1 step of the  $\text{Ca}^{2+}$  ATPase, the conformational changes of this step was determined by monitoring the  $\text{Ca}^{2+}$ -induced changes in fluorescence of  $\text{Ca}^{2+}$ -ATPase labelled with FITC [17]. This was measured upon the addition of  $400 \mu\text{M}$   $\text{Ca}^{2+}$  at pH 6,  $25^\circ\text{C}$  where the enzyme is predominately in the E2 form [17]. Figure 4 shows the effects of HBCD on FITC-labelled  $\text{Ca}^{2+}$ -ATPase when  $\text{Ca}^{2+}$  is added. The addition of  $\text{Ca}^{2+}$  leads to a decrease in fluorescence of 7% in the absence of HBCD corresponding to the ATPase shifting from an E2 state to the  $\text{Ca}^{2+}$  bound E1 state. In the presences of 2 and  $10\mu\text{M}$  HBCD, the fluorescence change was reduced to 4.6% and 0.8%, respectively. Also the rate of change in the presence  $2 \mu\text{M}$  HBCD was considerably reduced compared to control. These results indicate that HBCD binds to  $\text{Ca}^{2+}$ -ATPase, stabilizing it in the E2 conformational state and dramatically slowing down its transition from the E2 to E1 states.

## 4.0 Discussion

In previous studies by our group we have shown that HBCD and TBBPA are able to induce cell death in a number of cell types via apoptosis through the intrinsic pathway, as determined by mitochondrial membrane depolarization, mitochondrial release of cytochrome c, and activation of caspase 9 [8, 11]. All of these processes occur at similar concentration ranges, which also cause transient increases in intracellular  $[\text{Ca}^{2+}]$  (in the presence or absence of external  $\text{Ca}^{2+}$ ), as well as inhibition of SR /ER  $\text{Ca}^{2+}$  ATPase activity, which are factors known to induce intrinsic apoptosis through the processes highlighted above [2,8,11,20]. These observations therefore lead us to conclude that acute exposure of cells to HBCD and TBBPA, causes cell death through inhibiting the SERCA  $\text{Ca}^{2+}$  pumps. Here we have extended the range of BFRs studied and again show a direct correlation between potency at inducing cell death and potency at inhibition SERCA, suggesting that SERCA

inhibition is a major molecular mechanism by which acute exposure to a diverse range of BFRs causes cell death.

HBCD is shown to be a potent inhibitor of both the SERCA 1A and SERCA 2B isoforms of  $\text{Ca}^{2+}$  ATPase, with very similar  $\text{IC}_{50}$  values, indicating that this inhibition is isoform-independent. Furthermore, of all the BFRs tested within this study, HBCD proved to be the most potent inhibitor of the SERCA so far reported. Although the SERCA  $\text{Ca}^{2+}$  pump is the most abundant type of  $\text{Ca}^{2+}$  ATPase found in mammalian cells, it cannot be ruled out that HBCD and other BFRs also inhibit other  $\text{Ca}^{2+}$ ATPases within cells, as we have recently shown that TBBPA can inhibit the Golgi  $\text{Ca}^{2+}$  ATPase (SPCA1) [21].

In order to elucidate the molecular mechanism by which HBCD inhibits the  $\text{Ca}^{2+}$  ATPase a detailed enzymological study was undertaken using the highly abundant and easily purified skeletal muscle  $\text{Ca}^{2+}$  ATPase (SERCA 1A) isoform, which shows the same mechanism and has similar inhibitor properties to that of SERCA 2B [16,20]. The catalysis and transport mechanism of SERCA is complex and involves alternation between two major conformational states, known as E1(which is a high affinity  $\text{Ca}^{2+}$  binding state) and E2 (which is a low affinity  $\text{Ca}^{2+}$  binding state) [22] driven by transient auto-phosphorylation steps (see fig. 5) .

From the activity versus [ATP] data in fig. 2B, it was inferred that HBCD could potentially be affecting the affinity for ATP binding. This is further supported in fig. 3 by  $^{32}\text{P}$ -ATP phosphorylation studies which also showed a reduction in ATP-dependent phosphorylation consistent with a decrease in ATP affinity of the  $\text{Ca}^{2+}$  ATPase (step A in fig. 5). One possibility to explain this is that HBCD binds at or close to the nucleotide binding domain of the  $\text{Ca}^{2+}$  ATPase, occluding ATP from binding. However, HBCD is unlikely to have any effect on the affinity for  $\text{Ca}^{2+}$  binding to the E1 form and E2 form of the  $\text{Ca}^{2+}$ -ATPase (fig. 2A) or on the affinity for  $\text{Mg}^{2+}$  binding (fig. 2C) as no major changes in the kinetic constants was observed with these ions in the presence or absence of HBCD.

In previous studies investigating the effects of hydrophobic inhibitors on the activity of the  $\text{Ca}^{2+}$  ATPase such as nonylphenol, BHQ and TBBPA, we demonstrated that

one of the key steps affected was the E2-E1 transition [2,17,20]. In this study we also showed similar results, indicating that HBCD also stabilizes the  $\text{Ca}^{2+}$  ATPase in an E2 conformation by affecting both the E1 / E2 equilibrium position and rate at which the ATPase proceeds from the E2 state back to the E1 (step B in fig. 5). It has been previously shown that small inhibitors like BHQ, which also stabilizes the E2 state [20], bind within a hydrophobic cavity within the transmembrane domain formed by helices 1, 3 and 4 [2,20], which may also be where HBCD could bind.

In this study we have used commercial grade HBCD which consists of 3 main isomers ( $\alpha$ ,  $\beta$  and  $\gamma$ ) [23], with the most abundant of these isomers being  $\gamma$  (~82%) followed by  $\alpha$  (~12%). Recent studies have shown that the  $\alpha$  isomer seems to be preferentially absorbed within the brains of mice, while juvenile mice can accumulate detectable levels of both  $\alpha$  and  $\gamma$  [24, 25]. Therefore future studies would need to determine whether these different isomers have different potencies at inhibiting SERCA and causing cell death.

## **5.0 Conclusion**

In summary, there appears to be a good direct correlation for a number of unrelated BFRs including HBCD, between their potency at inducing cell death in SH-SY5Y neuronal cells and their ability to inhibit the activity of their SERCA  $\text{Ca}^{2+}$ -ATPase. This correlation is likely to indicate that, at least for some BFRs, acute toxicity is likely to be through inhibition of SERCA and disturbance of intracellular  $\text{Ca}^{2+}$  homeostasis. The molecular mechanism by which HBCD inhibits the  $\text{Ca}^{2+}$  ATPase is by altering ATP binding / phosphorylation and affecting the E2 to E1 transition step.

## **Acknowledgements**

The Ministry of Health, Saudi Arabia is thanked for a PhD scholarship to F. Al-Mousa. Dr Al-Mousa is currently assistant director for poison control and forensic chemistry, Ministry of Health, Riyadh, Saudi Arabia. There are no known conflicts of interest.

## **References**

- [1] M.J. Berridge, M.D. Bootman, P. Lipp, Calcium: a life and death signal, *Nature* 395 (1998) 645-648
- [2] O.A. Ogunbayo, F. Michelangeli, The widely utilized brominated flame retardant tetrabromobisphenol A (TBBPA) is a potent inhibitor of the SERCA  $\text{Ca}^{2+}$  pump, *Biochem. J.* 408 (2007) 407-415
- [3] T. Reistad, F. Fonnum, E. Mariussen, Neurotoxicity of the pentabrominated diphenyl ether mixture, DE-71, and hexabromocyclododecane (HBCD) in rat cerebellar granule cells in vitro, *Arch Tox.* 80 (2006) 785-796
- [4] M. Remberger, J. Sternbeck, A. Palm, L. Kaj, K. Stromberg, E. Brorstrom-Lunden, The environmental occurrence of hexabromocyclododecane in Sweden, *Chemosphere* 54 (2004) 9-21
- [5] A. Corvaci, A.C. Gerecke, R.J. Law, S. Voorpoels, M. Kohler, N.V. Heeb, H. Leslie, C.R. Allchin, J. DeBoer, Hexabromocyclododecanes (HBCD) in the environment and humans: a review, *Environ. Sci. Technol.* 40 (2006) 3679-3688
- [6] C. Thomsen, P. Molander, H.L. Daae, K. Janak, M. Froshaug, V.H. Liane, S. Thorud, G. Becher, E. Dybing, Occupational exposure to hexabromocyclododecane at an industrial plant, *Environ. Sci. Technol.* 41 (2007) 5210-5216
- [7] Z. Shi, Y. Jiao, Y. Hu, Z. Sun, X. Zhou, J. Feng, J. Li, Y. Wu, Levels of tetrabromobisphenol A, hexabromocyclododecanes and polybrominated diphenyl ethers in human milk from the general population in Beijing, China, *Sci. Total Environ.* 1 (2013) 452-453
- [8] F. Al-Mousa, F. Michelangeli, some commonly used brominated flame retardants cause  $\text{Ca}^{2+}$ -ATPase inhibition, beta-amyloid peptide release and apoptosis in SH-SY5Y neuronal cells, *PLOS one* 7 (2012) e33059
- [9] A.L. Williams, J.M. Desesso, The potential of selected brominated flame retardants to affect neurological development, *J. Toxicol. Environ. Health B. Crit. Rev.* 13 (2010) 411-448
- [10] P.J. Hughes, H. McLellan, D.A. Lowes, S.Z. Khan, J.G. Bilemen, S.C. Tovey, R.E. Godfrey, R.H. Michell, C.J. Kirk, F. Michelangeli, Estrogenic alkylphenols induce cell death by inhibiting testis endoplasmic reticulum  $\text{Ca}^{2+}$  pumps, *Biochem. Biophys. Res. Comm.* 277 (2000) 568-574
- [11] O.A. Ogunbayo, P.F. Lai, T.J. Connolly, F. Michelangeli, Tetrabromobisphenol A (TBBPA) induces cell death in TM4 Sertoli cells by modulating  $\text{Ca}^{2+}$  transport

proteins and causing dysregulation of  $\text{Ca}^{2+}$  homeostasis, *Toxicol. In Vitro.* 22 (2008) 943-952

[12] T. Hassenklover, S. Predehl, J. Pilli, J. Ledwolovz, M. Assmann, U. Bickmeyer, Bromophenols both present in marine organisms and in industrial flame retardants, disturb cellular  $\text{Ca}^{2+}$  signalling in neuroendocrine cells (PC12), *Aquat. Toxicol.* 76 (2006) 37-45

[13] M.M. Dingemans, H.J. Heusinkveld, A. de Groot, A. Bergman, M. Van den Berg, R.H. Westerink, Hexabromocyclododecane inhibits depolarisation-induced increase in calcium levels and neurotransmitter release in PC 12 cells, *Toxicol Sci.* 107 (2009) 490-497

[14] F. Michelangeli, F.M. Munkonge, Methods of reconstitution of the purified sarcoplasmic reticulum ( $\text{Ca}^{2+}$ - $\text{Mg}^{2+}$ )-ATPase using bile salt detergents to form membranes of defined lipid to protein ratios or sealed vesicles, *Anal. Biochem.* 194 (1991) 231-236

[15] F. Michelangeli, J. Colyer, J.M. East, A.G. Lee, Effect of pH on the activity of the  $\text{Ca}^{2+}$ - $\text{Mg}^{2+}$ -activated ATPase of sarcoplasmic reticulum, *Biochem. J.* 267 (1990) 423-429

[16] L.L. Wootton, F. Michelangeli, The effects of the phenylalanine 256 to valine mutation on the sensitivity of the sarcoplasmic / endoplasmic reticulum  $\text{Ca}^{2+}$  ATPase (SERCA)  $\text{Ca}^{2+}$  pump isoforms 1,2, and 3 to thapsigargin and other inhibitors, *J. Biol. Chem.*, 281 (2006) 6970-6976

[17] F. Michelangeli, S. Orłowski, P. Champeil, J.M. East, A.G. Lee, Mechanism of inhibition of the ( $\text{Ca}^{2+}$ - $\text{Mg}^{2+}$ )-ATPase by nonylphenol, *Biochemistry*, 29 (1990) 3091-3101

[18] L. Brunello, E. Zampese, C. Floren, T. Pozzan, P. Pizzo, C. Fasolato, Presenilin 2 dampens intracellular  $\text{Ca}^{2+}$  stores by increasing  $\text{Ca}^{2+}$  leakage and reducing  $\text{Ca}^{2+}$  uptake, *J. Cell Mol. Med.* 13 (2009) 3358-3369

[19] R.C. Duggleby, J.M. East, A.G. Lee, Luminal dissociation of  $\text{Ca}^{2+}$  from the phosphorylated  $\text{Ca}^{2+}$ -ATPase is sequential and gated by  $\text{Mg}^{2+}$ , *Biochem. J.* 339 (1999) 351-357

[20] F. Michelangeli, J.M. East, A diversity of SERCA  $\text{Ca}^{2+}$  pump inhibitors, *Biochem. Soc. Trans.*, 39 (2011) 789-797

- [21] P.F. Lai, F. Michelangeli, Bis(2-hydroxy-3-tert-butyl-5-methyl)-methane (bisphenol) is a potent and selective inhibitor of the secretory pathway  $\text{Ca}^{2+}$  ATPase (SPCA1), *Biochem. Biophys. Res. Comm.* 424 (2012) 616-619
- [22] L. DeMeis, A.L. Vianna, Energy interconversion by the  $\text{Ca}^{2+}$ -dependent ATPase of the sarcoplasmic reticulum, *Annu. Rev. Biochem.* 48 (1979) 275-292
- [23] N.V. Heeb, W.B. Schweizer, M. Kohler, A.C. Gerecke, Structure elucidation of hexabromocyclododecane—a class of compounds with complex stereochemistry, *Chemosphere* 61 (2005) 65-73
- [24] D.T. Szabo, J.J. Diliberto, J.K. Huwe, L.S. Birnbaum, Differences in tissue distribution of HBCD alpha and gamma between adult and developing mice, *Toxicol. Sci.*, 123 (2011) 256-263
- [25] H. Hakk, D.T. Szabo, J. Huwe, J. Diliberto, L.S. Birnbaum, Novel and distinct metabolites identified following a single oral dose of  $\alpha$ - or  $\gamma$ -hexabromocyclododecane in mice, *Environ. Sci. Technol.* 46 (2012) 13494-13503

### **Conflict of Interest Statement**

The authors declare that there is no conflict of interest.

### **Figure Captions**

#### **Figure 1: Inhibition of the $\text{Ca}^{2+}$ ATPase by HBCD and other BFRs and their correlation with cell viability.**

(A) Shows the inhibition of HBCD on the  $\text{Ca}^{2+}$  ATPase activity, measured as a % of control, in microsomal membranes isolated from SH-SY5Y cells ( $\blacktriangle$ ) and skeletal muscle SR  $\text{Ca}^{2+}$  ATPase ( $\blacksquare$ ). The data points represent the mean  $\pm$  S.D. of 3 to 5 determinations. (B) Shows the correlation for a number of BFRs between the potency of inhibition of the  $\text{Ca}^{2+}$  ATPase activity from SH-SY5Y cells ( $\text{IC}_{50}$ ), with their potency at causing SH-SY5Y cell death ( $\text{LC}_{50}$ ). The data points and error bars were determined from  $\text{Ca}^{2+}$  ATPase inhibition and cell viability profiles versus [BFR], with each data point representing the mean  $\pm$  S.D. of 3 to 5 determinations. The BFRs used in this study were: Hexabromocyclododecane (HBCD), Tetrabromobisphenol-A

(TBBPA), Decabromodiphenyl ether (DBPE), Tetrabromobisphenol-A-diallyl ether (TBBPA-DAE), Dibromobiphenyl (DBBP), Pentabromodiphenyl ether (PBDE) and Octabromodiphenyl ether (OBDE).

**Figures 2: The effects of HBCD on the SR (SERCA 1A)  $\text{Ca}^{2+}$  ATPase activity as a function of free  $[\text{Ca}^{2+}]$ ,  $[\text{ATP}]$  and  $[\text{Mg}^{2+}]$ .**

All experiments were undertaken at pH 7.2 and 25°C in the absence (■) or presence (▲) of 3  $\mu\text{M}$  HBCD. Each data point is the mean  $\pm$  S.D. of 3 - 5 determinations.

(A) Shows the effect of free  $[\text{Ca}^{2+}]$  on the ATPase activity in the presence or absence of 3  $\mu\text{M}$  HBCD. (B) Shows the effect of a range of  $[\text{ATP}]$  on the ATPase activity in the presence and absence of 3  $\mu\text{M}$  HBCD. (C) Shows the effects of  $[\text{Mg}^{2+}]$  on the ATPase activity in the presence or absence of 3  $\mu\text{M}$  HBCD.

**Figure 3: The effects of HBCD on  $[\text{}^{32}\text{P}]$  ATP-dependent phosphorylation of the  $\text{Ca}^{2+}$  ATPase.**

All phosphorylation experiments were undertaken at pH 7.2 and 25°C and each data point represents the mean  $\pm$  S.D. of 3 determinations. The level of ATP-dependent phosphorylation was measured in the absence (■) or presence (▲) of 10  $\mu\text{M}$  HBCD, over a range of ATP concentrations (0-20  $\mu\text{M}$ ).

**Figure 4: The effects of HBCD on the E2 to E1 step of the  $\text{Ca}^{2+}$  ATPase.**

The traces represent changes in fluorescence of FITC-labelled  $\text{Ca}^{2+}$  ATPase upon addition of 400  $\mu\text{M}$   $\text{Ca}^{2+}$ , when undertaken in a buffer at pH 6.0. The experiments were undertaken either in the absence of HBCD (con), or in the presence of 2  $\mu\text{M}$  and 10  $\mu\text{M}$  HBCD. The traces shown are individual experiments which are representative of 3 separate experiments.

**Figure 5: The  $\text{Ca}^{2+}$  ATPase mechanism.**

The figure shows the mechanism by which the  $\text{Ca}^{2+}$  ATPase transports  $\text{Ca}^{2+}$  and hydrolyses ATP, and highlights the steps (ATP binding; A, and the E2 to E1 transition; step B) that are proposed to be altered in the presence HBCD.



Figure 1

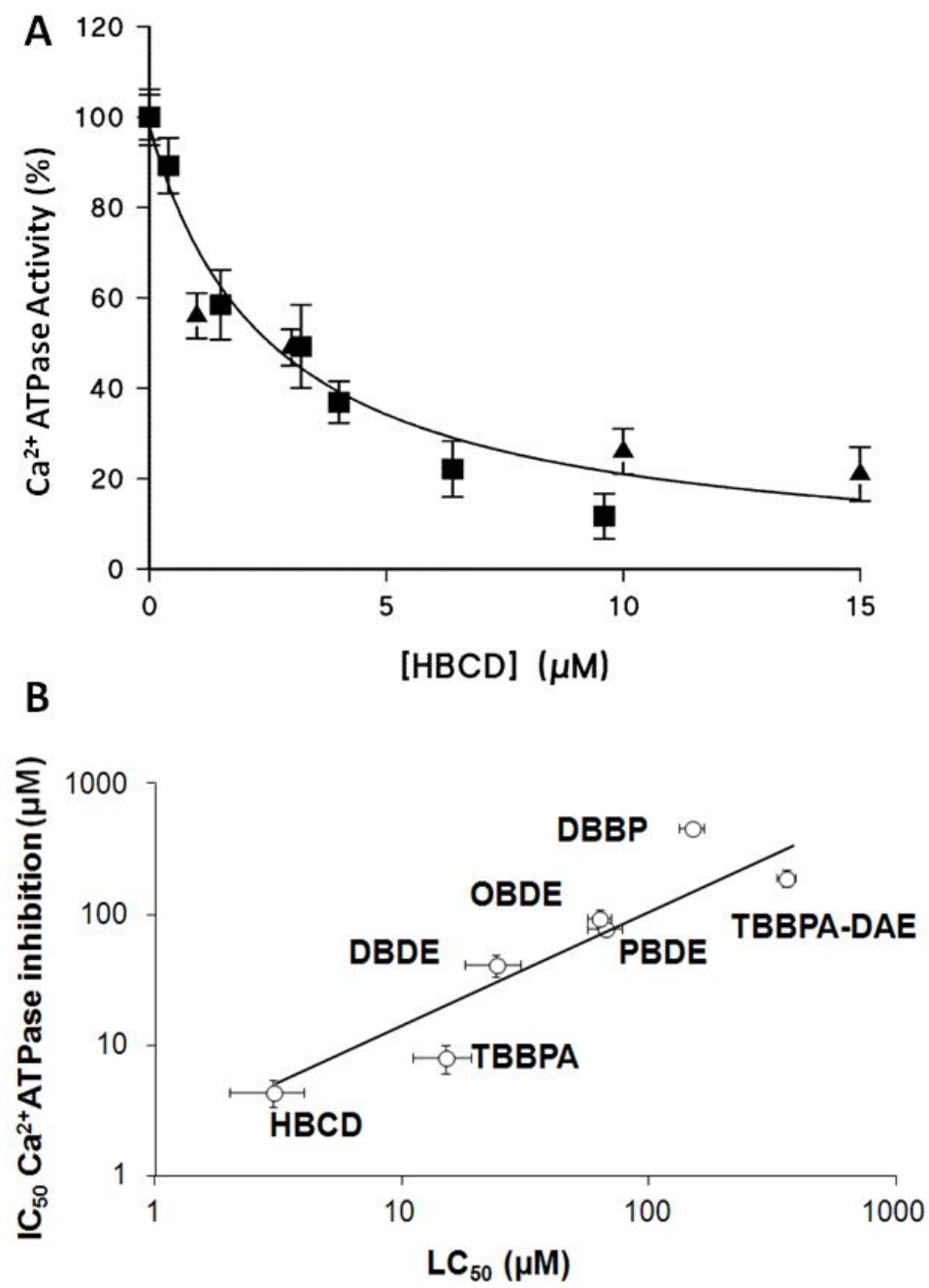


Figure 2

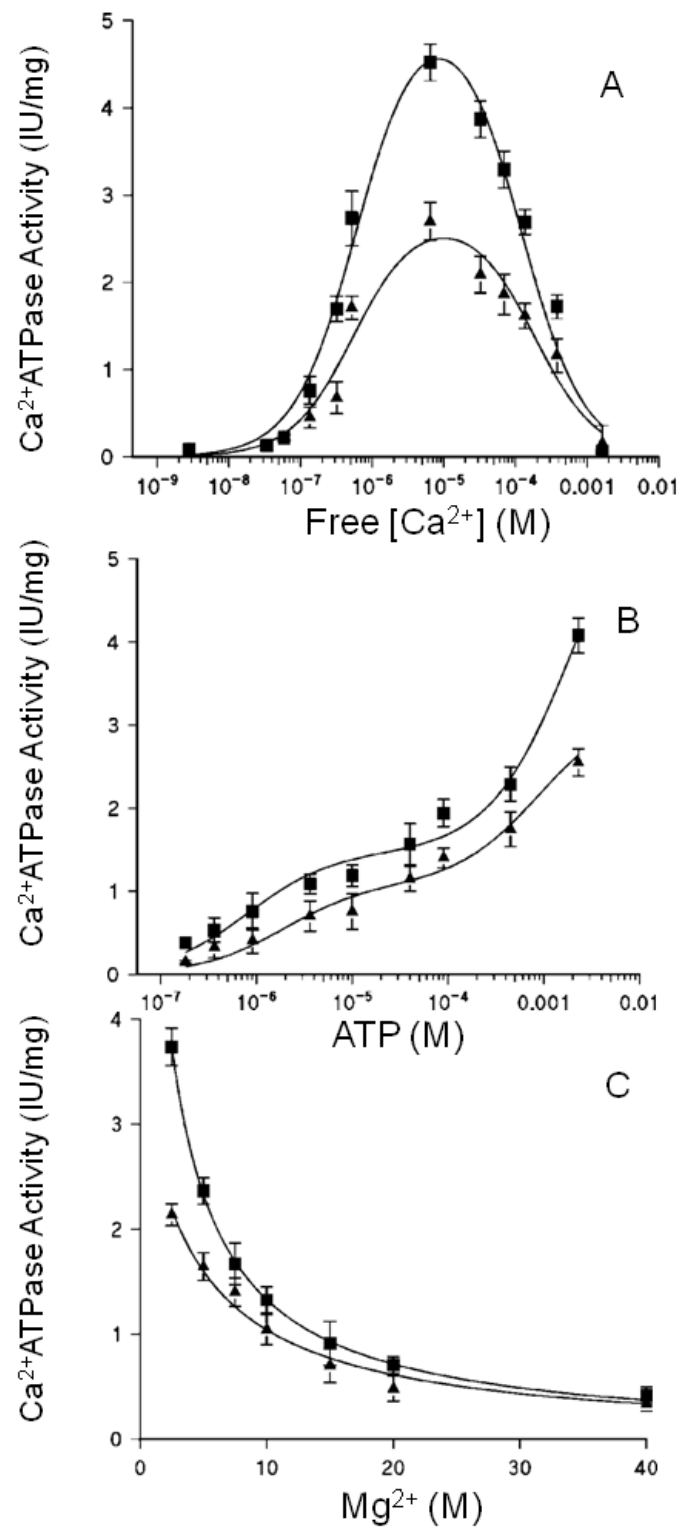


Figure 3

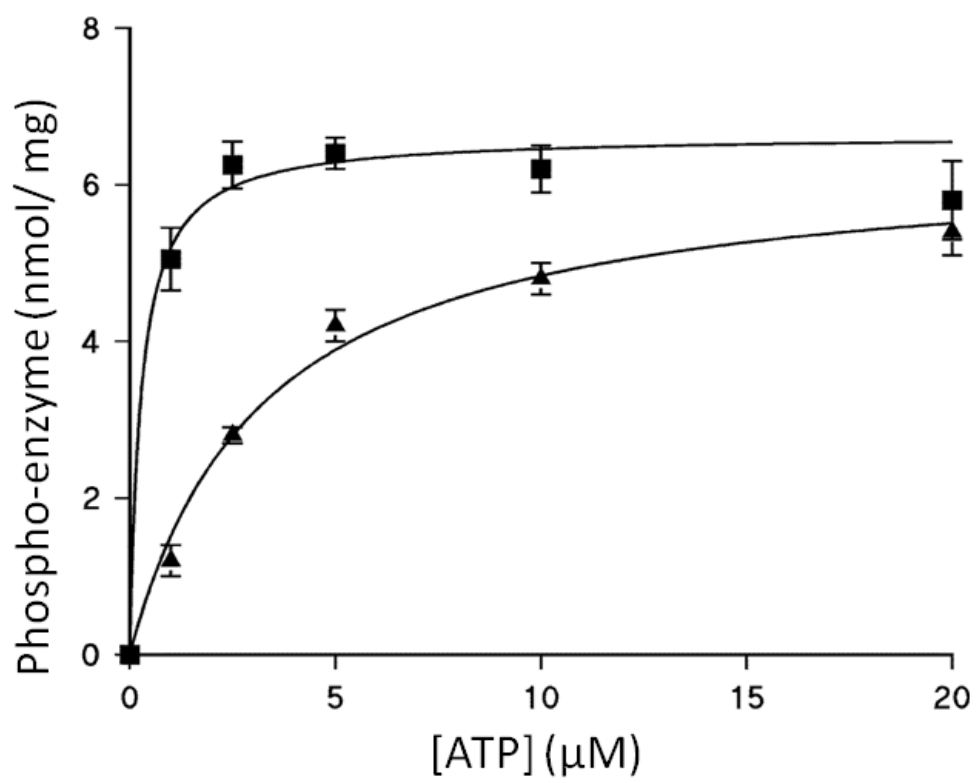


Figure 4

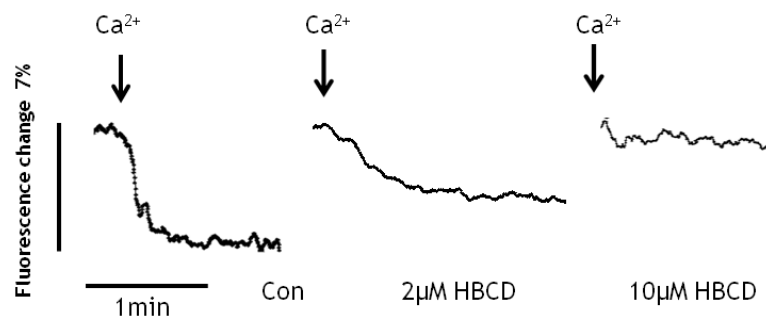


Figure 5

